Similarity Check-Short and Open Circuit Fault Detection in On Grid Photovoltaic Systems

by Ta IKetut

| RESEARCH ARTICLE

Short and Open Circuit Fault Detection in On-Grid Photovoltaic Systems 1MWP Bangli Based on Current and Voltage Observation

IBK Sugirianta[1] ✉ **IGNA Dwijaya_S[2], M Purbhawa[3], GK Sri Budarsa[4] and Ketut Ta[5]**
[12345]*Departement of Electrical Engineering, Politeknik Negeri Bali, Bali, Indonesia*
Corresponding Author: IBK Sugirianta, **E-mail**: ibksugirianta@pnb.ac.id

| ABSTRACT

Photovoltaic (PV) systems as clean and green electrical energy generators have increased sharply in the last 10 years. The installation of a PV system in an open area is one of the causes of frequent faults/damage to the PV system. Fault in the PV system causes a decrease in efficiency, weak reliability, and disruption of the continuity of the electrical power distribution, which in turn causes the low performance of the system. This research does on the on-grid PV system 1MWp Bangli which consists of 278 PV arrays and 5004 monocrystalline solar modules 200Wp, which started operation in 2013. This research aims to find open circuit and short circuit faults that occur in the PV system Bangli. The method used in this research is the current and voltage observation method. Current and output voltage measurements from the PV array are carried out as well as measurements of working module temperature and solar irradiance. To calculate the output PV array's current (R_I) and voltage (R_V) indicators; Calculation of the current (R_{IM}) and voltage (R_{VM}) indicators under fault-free conditions, and the short circuit (T_{IO}) and open voltage (T_{VS}) threshold are calculated. As a result, this study succeeded in determining short and open circuit faults that occur in PV systems on grid 1MWp Bangli.

1. Introduction

Renewable energy is a form of energy developed as a clean and green future energy source. Among the various renewable energies, solar energy is one of the most attractive energy sources due to its technical, economic, and environmental benefits (Yi & Etemadi, 2017). Currently, solar or photovoltaic (PV) power generation is considered one of the most promising renewable energy sources because of its ability to produce clean energy for various applications (Fazai et al., 2019). In addition, solar energy is freely available in unlimited quantities and does not require moving parts to be converted into electrical energy (Kumar et al., 2018). Along with the development trend of power generation with renewable energy sources, the deployment of PV systems continues to increase (Chen & Wang, 2018). The percentage of solar power in the grid worldwide is increasing every year (Harrou et al., 2019). Worldwide, PV power generation has been increasing exponentially, with total installed capacity reaching more than 303 GW in 2016 from only 1.3 GW in 2000, accounting for at least 1.8% of the world's electricity demand. In Indonesia, through the National Energy General Plan (RUEN), a policy of increasing the share of renewable energy in the national energy mix to 23% by 2025. All of this shows the increasing use of solar (renewable) energy, which will continue to increase.

In its operation, PV systems installed openly in nature cannot be separated from damage and disturbances to the system. There are four types of disturbances that commonly occur in PV systems, namely (Chen et al., 2018): shadow (occurs when the surface of the PV module is blocked from sunlight), ground fault (unexpected connection between circuit and ground), line-line short circuit (the unexpected short circuit between two different potential points between the PV module or array), DC arc fault (triggered by

high voltage power discharge between different conductors) (Chen & Wang, 2018). Components of a PV system that may be affected by interference are panels, modules, arrays, connection lines, converters, and inverters (Fazai et al., 2019). Meanwhile, based on time characteristics, disturbances in PV systems can be grouped into three, namely: intermittent, sudden, or incipient (Fazai et al., 2019). A study conducted over two years in several PV systems in the UK showed that the annual energy loss caused by disturbances in such PV systems could account for 18.9% of the total capacity of a PV system (Firth et al., 2010). PV array system disturbances, be it shading, ground faults, short circuit lines, DC arcs, or degradation, can reduce PV power supply by around 22.34% to 27.58% (Lillo-Bravo et al., 2018). The above shows that the PV system cannot be separated from the influence of disturbances, and disturbances that occur can cause loss of power generated by the PV system.

This study discusses open and short circuit faults in the on-grid PV system Bangli. First, data collection from site condition and characteristic module PV. Second, data processing, calculation of measured current and voltage indicators, current and voltage indicators in fault-free operation, and calculation of an open circuit fault and short circuit fault threshold indicators are carried out. Third, observe the current and voltage indicator with fault threshold indicators. Fourth, we report the observation results of the open circuit and short circuit fault detection based on the observation of current and voltage measurement results.

2. Literature Review

Two common faults that may occur in the DC part of a PV system are short circuit faults and open circuit faults which have been studied in references (Garoudja et al., 2017) and (Mansouri et al., 2018). An open circuit fault can occur due to a series of breaks in the wires between the solar cells. An open circuit fault is shown at point 'F1' of the PV array in **Fig. 1**. Short-circuit faults are mainly caused by poor wiring in the PV strings or between the PV strings. In addition, aging, vibration, and abrasion of PV modules are also significant sources of short-circuit faults. When there are different faults in a PV array system, the output characteristics of the PV array will show other things, depending on the type of fault that occurs, as shown in **Fig. 2**. When an open circuit fault occurs in an array, the output current of the array will be significantly reduced; whereas when a short circuit occurs, the output voltage of the PV array will decrease rapidly.
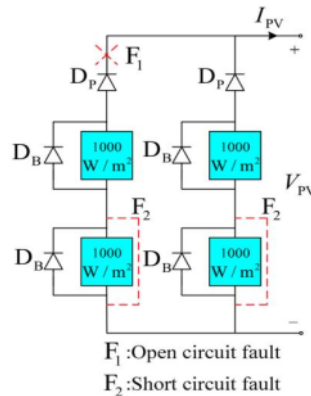
Fig 1. The configuration structure of the PV array under open circuit and short circuit faults (Pei and Hao, 2019)

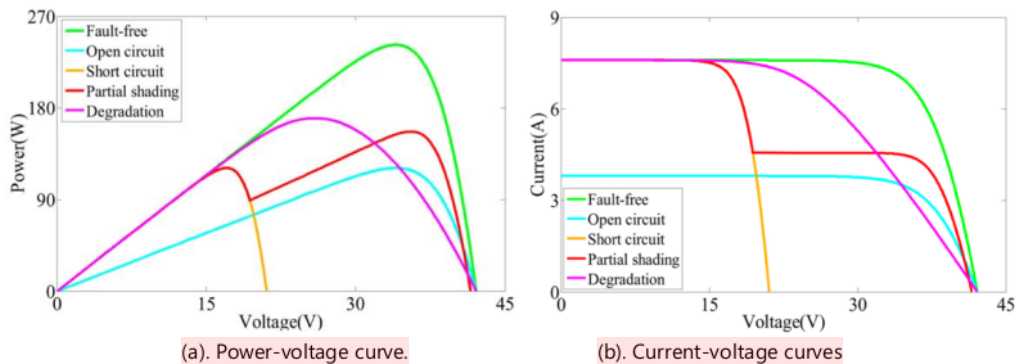(a). Power-voltage curve.   (b). Current-voltage curves

Fig 2. The output characteristic curve PV array under open circuit and short circuit fault. (a). Power-voltage curves, (b). Current-voltage curves (Pei and Hao, 2019)

3. Methodology

3.1 Site Condition and Equipment Photovoltaic Systems On-Grid 1MWp Bangli.

The Bangli 1MWp On-grid PLTS system is located in Kayubihi Village, Bangli District, Bangli Regency, Bali Province (-8.35, 115.36), and has been operating since 2013

Fig. 3 Satelit foto on-grid photovoltaic systems 1MWp Bangli

The main equipment and components of the on-grid PV system Bangli are as follows:

- 278 PV arrays, fixed support type.
- 5004 monocrystalline solar modules 200Wp.
- 50 unit combiner box (array protection panel)
- 50 unit 3-phase inverter string type 20 kW/unit.
- 5 unit distribution panels
- 5 unit step-up transformer, 230/400 V to 20 kV.
- Conventional lightning protection
- Remote monitoring system to display data and information.

3.2 PV Modul 200 Wp 24 Volt

There is a 5004 unit PV module 200Wp monocrystalline type installed in the on-grid photovoltaic system 1MWp Bangli. Monocrystalline 200 Wp PV module with a length and width of 1580 mm x 808 mm with a total of 72 cells per module.

Table 1
Electrical characteristics PV module 200Wp

Maximum power	200 Watt
Voltage at open circuit (Voc)	45,5 Volt
Current at short circuit (Isc)	5,80 Ampere
Voltage at the MPP	37,44 Volt
Current at the MPP	5,35 Ampere
Cell per module	72

Source: PV 200Wp name plate

3.3 PV Array Configuration

The Bangli PV system has 278 PV arrays connected to 50 combiner boxes (array protection panels). Each array protection panel consists of 5-6 PV arrays, each connected in parallel to serve a 200 Kw inverter. Furthermore, each PV array consists of 18 PV modules connected in series. Fig. 4 shows the configuration structure of an array protection panel. This panel is equipped with blocking diodes, over-current protection devices (OCPD), miniature circuit breakers (MCB), and surge protection devices (SPD).
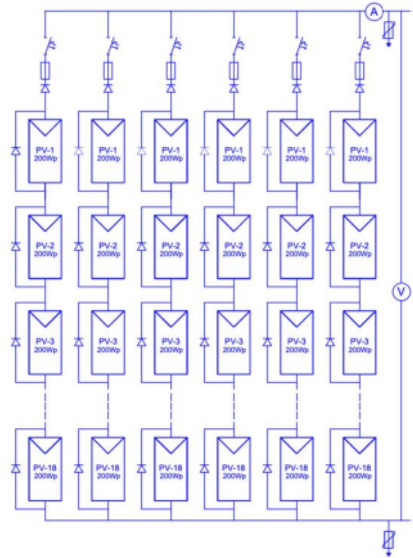
Fig. 4 The configuration structure of the photovoltaic (PV) array in the array protection panel PV system Bangli.

3.4 Definition Voltage and Current Indikator

In this study, two types of faults are detected, namely short circuit faults and open circuit faults. First, get the current and voltage indicators by utilizing the results of current and voltage measurements along with the value of the short circuit current and the open circuit voltage value of the PV array. The PV current and voltage indicators can be defined as follows: (Silvestre et al., 2014):

$$R_V = \frac{V}{V_{oc}} \tag{1}$$

$$R_I = \frac{I}{I_{sc}} \tag{2}$$

Where R_I and R_V are current and voltage indicators PV system, respectively; I and V are the results of measuring the current and output voltage of the PV array, respectively; Isc and Voc are the short-circuit current and the open-circuit voltage PV array and are given separately as follows (Silvestre et al., 2014):

$$I_{sc} = N_p \left(\frac{I_{scm\_STC}}{1000} G + K_I (T - T_{STC}) \right) \tag{3}$$

$$V_{oc} = N_s \left(V_{ocm\_STC} + K_V (T - T_{STC}) + V_t \ln \left(\frac{I_{sc}/N_p}{I_{scm\_STC}} \right) \right) \tag{4}$$

Where Np is the number of the PV strings of the PV array; Ns is the number of the PV modules of a PV string; Iscm_STC is the short-circuit current of the PV module at Standard Test Conditions (irradiation: G_{STC}=1000W/m2, temperature: T_{STC}=25°C); V_{ocm_STC} is the open circuit voltage of the PV module at standard test conditions; K_I, K_V is temperature coefficients of the short-circuit current and the open-circuit voltage, respectively; G is the PV module receiving irradiation and T is the PV module temperature; Vt is the thermal voltage of the PV module. According to Equations (3) and (4), the voltage and current indicators of the PV system in fault-free operation can be expressed by (Silvestre et al. 2014):

$$Rvm=Vm/Voc \tag{5}$$

$$Rim=Im/Isc \tag{6}$$

Where R_{IM} and R_{VM} are the current and voltage indicators of the PV system in fault-free operation, respectively; Im and Vm are the output voltage and current at the MPP of the PV array during the fault-free condition and are separately given (Silvestre et al. 2014):

$$I_m = N_P\left(\frac{I_{mm\_STC}}{1000}G + K_I(T - T_{STC})\right) \qquad (7)$$

$$V_m = N_s\left(V_t \ln\left(1 + \frac{I_{sc} - I_m}{I_{sc}}(e^{\frac{V_{oc}}{N_s V_t}} - 1)\right) - \frac{I_m}{N_P}R_s\right) \qquad (8)$$

Where Imm_STC is the current at the MPP of the PV module at Standard Test Conditions, Rs is the series equivalent resistance of the PV module.

3.5. Fault Detection Threshold
3.5.1. Open Circuit Fault
In a combiner box consisting of several strings, when an open circuit fault occurs on a string, the amount of current that comes out of the circuit will decrease by the current value that should be flowed by the circuit that ignores the open circuit. In this state, the current indicator can be calculated as follows: (Yahyaoui and Segatto 2017):

$$R_{IO} = ((N_P-1))/N_P \ I_m/I_{sc} = \alpha \ R_{IM.} \qquad (9)$$

Where R_{IO} is the current indicator when an open circuit fault exists in the PV array; α is given as:

$$\alpha = 1 - 1/N_P \qquad (10)$$

Therefore, the fault detection threshold of open circuit faults are be defined by (Yahyaoui and Segatto 2017):

$$T_{IO} = \varepsilon\alpha RIM \qquad (11)$$

Where ε is fault detection allowed correction coefficient, which consists of two factors, the degradation factor, and measurement tolerance, the degradation factor for PV is 1% per year, and the measurement tolerance is 3%. PV Bangli has been operating for nine years, ε=-12%. T_{IO} is an open-circuit fault threshold, and when one or more PV strings are subjected to an open-circuit fault, the R_I given in equation (4) will be below the T_{IO}.

3.5.2. Short Circuit Fault
When the PV module on the string is short-circuited, the voltage on the string will be reduced by the voltage of the short-circuited PV module. Based on this situation, the voltage indicator can be calculated as follows (Yahyaoui & Segatto, 2017):

$$R_{VS} = \frac{(N_s-1)}{N_s}\frac{V_m}{V_{oc}} = \beta \ R_{VM} \qquad (12)$$

Where R_{VS} is the voltage indicator when a short-circuited PV module is present in one of the PV strings; β is given as:

$$\beta = 1 - \frac{1}{N_s} \qquad (13)$$

Therefore, the fault detection threshold of short-circuit faults are be defined by (Yahyaoui & Segatto, 2017):

$$T_{VS} = \varepsilon\beta R_{VM} \qquad (14)$$

Where T_{VS} is the short-circuit fault threshold, and when one or more PV modules in a string are short-circuited, the R_V value given in equation (3) will be below than T_{VS}.

3.5.3 Degradation
The level of energy production from solar panels is determined mainly by the level of degradation of the PV module. Studies that have been carried out (Sangwongwanich et al., 2018) show that the level of PV degradation varies and is determined mainly by the location of the PV installation. The degree of variation of PV degradation is strongly influenced by the climate in which the PV is installed. The results of studies (D. C. Jordan & Kurtz, 2013) (Dirk C. Jordan et al., 2016) show that the degradation will be faster under dry climate conditions than PV installed in cold climate conditions. In addition, the PV factory has also determined the level of degradation of the PV it produces, which ranges from 0.5 - 1% per year.

3.6. Application of Proposed Approach in the PV Array Fault Detection

Measurement of array output current, PV array output voltage, and voltage PV string, as well as temperature and solar radiation. In this study, fault detection at the Bangli PV power system was carried out using current and voltage analysis methods. As shown in Figure 1, on 39 units of combiner boxes, measurements were carried out in the field directly. The application of the proposed current and voltage observation method in error detection for PV arrays is implemented in the following process.
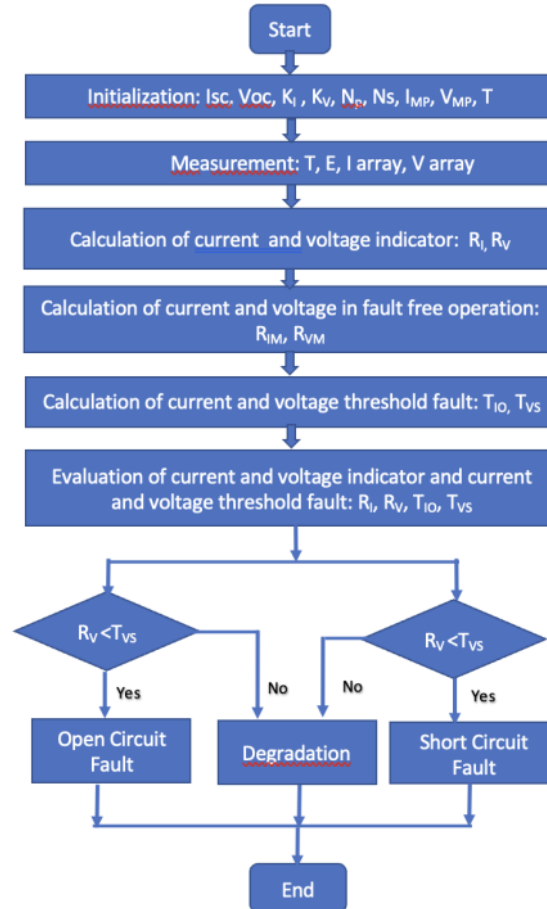

Fig 5. Flowchart of the proposed fault detection method

Step1 Initialization parameter: number of strings (Np) of PV array PV; the number of PV modules (Ns) in the string; characteristics of the PV Module. Current measurement data, (I) voltage (V), solar radiation (G), and working temperature (T) from the PV module

Step2 do the calculation. Calculation of the magnitude of the fault characteristics: open circuit voltage and short circuit current from PV Array (Voc, Isc); calculation of current and voltage indicators at the time of measurement (R_I, R_V), calculation of output voltage and current on the PV array in fault-free operation (Vm, Im); current and voltage indicators in fault-free conditions (R_{IM}, R_{VM}).

Step 3 Fault threshold calculation: first, the calculation of the open circuit PV Array (R_{IO}) fault current indicator and the short-circuit fault voltage indicator on one of the strings (R_{VS}). Then, according to equations (11) and (14), the T_{IO} and T_{VS} fault detection threshold is calculated.

Step 4 Evaluation of current and voltage indicators; first, evaluate the fault current and fault voltage indicators from the measurement results (R_I, R_V), then evaluate the threshold value for open circuit and short circuit faults (T_{IO}, T_{VS}).

Step 5 Fault detection: according to the fault detection principle, R_I will be compared with T_{IO} and R_V compared with T_{VS} at the same time so that this goal can be achieved to detect faults and identify the types of faults detected.

4. Results and Discussion
4.1 Measurement of current, voltage, solar irradiance, and temperature in PV array

In the Bangli PV system, 5004 units of 200 Wp modules are installed, making up 278 arrays, with 18 PV modules per array. They are connected to 50 units of 20 kVA inverter and combiner box. Currently, out of 50 inverter units, 11 units are damaged. The inverter unit that was damaged was the inverter/combiner box A5, B7, B8, C2, D1, D5, D6, D10, E1, E2, and E5. So only 39 inverter units operate. Measurements of voltage, current, temperature, and solar radiation were carried out for two weeks (late August-early September 2022) on 39 combiner box units serving 39 inverters. The measurement results are shown in Table 2 and Fig 6.a.b.c.d.

Table 2. Measurements of voltage, current, temperature, and solar irradiance

Comb. box	V array (V)	I array (A)	T module (C⁰)	Irradiance (W/m²)
E9	472	4,4	23	169
E6	489	4,1	30	183
E3	583	4,6	25	143
E8	591	6,9	27	259
E10	628	8,4	27	275
D3	636	7,0	28	277
E4	496	247,8	29	279
C6	351	8,2	43	297
B2	600	7,7	32	343
A10	619	9,1	28	351
D9	499	10,6	33	369
E7	630	7,4	26	377
B3	617	7,0	32	405
B1	594	9,6	35	421
D7	513	12,6	30	453
C4	601	8,3	37	463
D4	600	14,5	25	463
A6	296	10,8	30	473
A1	617	12,8	33	502
C5	592	13,2	45	536
C3	574	14,1	50	600
C10	584	13,2	38	626
B6	578	14,5	32	654
C9	509	19,1	48	695
C7	587	15,8	28	742
A8	591	17,0	30	746
D2	511	20,9	33	880
A9	587	17,8	42	897
A2	530	25,7	56	972
B9	304	22,0	47	984
A7	519	25,7	33	1146
B4	601	22,9	32	1158
C8	544	25,0	60	1251
C1	568	30,4	45	1294
A4	566	28,7	45	1321
A3	582	31,6	49	1357
B5	574	28,8	48	1426

Comb. box	V array (V)	I array (A)	T module (C⁰)	Irradiance (W/m²)
B10	509	30,2	54	1498
D8	584	36,7	43	1604

Fig. 6 (a), (b), (c), (d) is the display of data from the measurement of voltage, current, temperature, and solar irradiance, which has been sorted from the smallest value to the most significant value. **Fig. 6** (a) for voltage measurement ranges from 296 Volt to 636 Volt. The current measurements, **Fig. 6** (b), range between 4.1 amperes and 36.7 amperes. Temperature module measurement results **Fig. 6** (c), ranging from 230C to 600C. Meanwhile, the solar irradiance measurement ranges between 169 watts/m2 and 1604 watts/m2, **Fig. 6** (d).

(a). voltage array

(b). current array
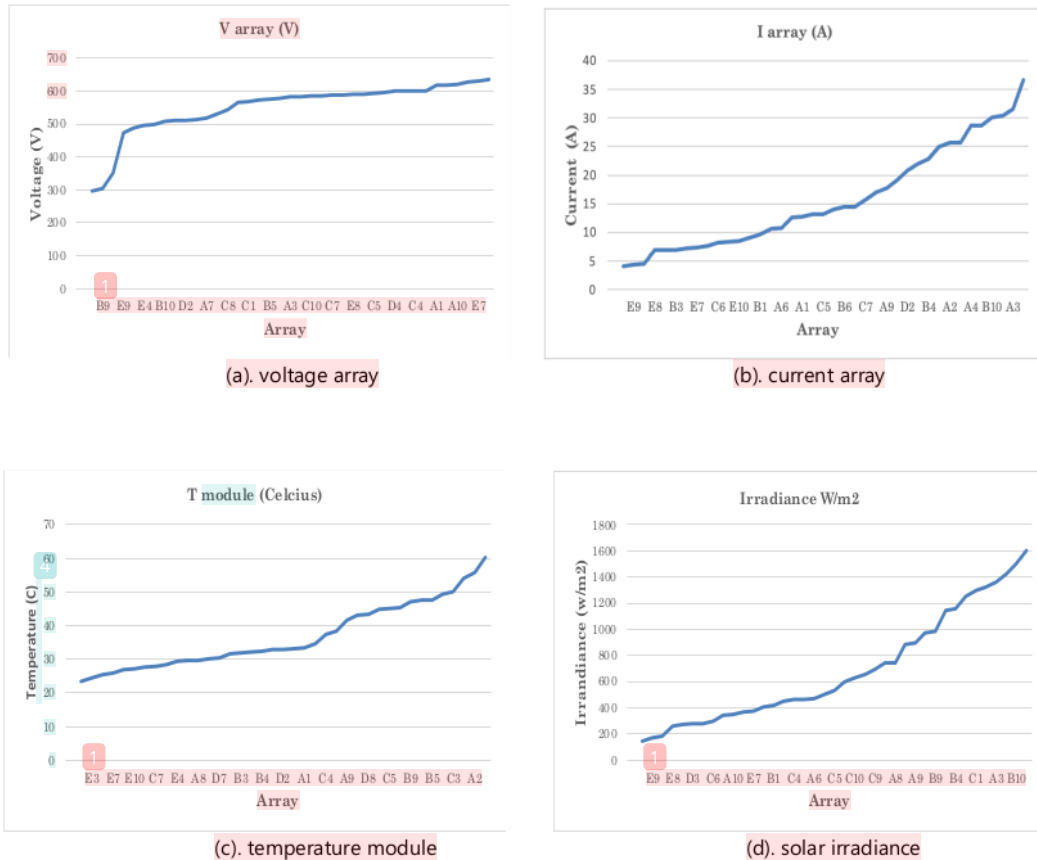
(c). temperature module

(d). solar irradiance

Fig 6. Range of PV array measurement result
(a). voltage array, (b). current array (c). temperature module (d). solar irradiance

4.2 Open Circuit Fault Observation and Detection

For the observation and detection of open circuit faults, from all the data that has been collected then, calculations are carried out using the equation (2), (3), (6), (7), (9), (10), (11) so that the results are as shown in Table 3. The results were obtained from 39 unit boxes combiner, and it was detected that an open circuit fault (OCF) occurred in ten combiner box units, namely the combiner boxes A3, B3, B5, C1, C3, C4, C7, C8, C10, and D8. In this case, the analysis results show that the value of the current measurement indicator is smaller than the open circuit fault threshold.

Table 3. Result of observation and detection of an open circuit fault

Box. comb.	RI	RIM	RIO	TIO	Result
A1	0,731	0,922	0,768	0,676	degr.
A2	0,758	0,921	0,767	0,675	degr.
A3	0,668	0,921	0,768	0,676	OCF
A4	0,748	0,922	0,737	0,649	degr.
A6	0,787	0,922	0,738	0,649	degr.
A7	0,773	0,922	0,738	0,649	degr.
A8	0,787	0,922	0,738	0,649	degr.
A9	0,683	0,921	0,737	0,649	degr.
A10	0,747	0,922	0,768	0,676	degr.
B1	0,785	0,921	0,737	0,649	degr.
B2	0,769	0,921	0,737	0,649	degr.
B3	0,602	0,922	0,737	0,649	OCF
B4	0,681	0,922	0,738	0,649	degr.
B5	0,579	0,922	0,768	0,676	OCF
B6	0,763	0,922	0,738	0,649	degr.
B9	0,771	0,921	0,737	0,649	degr.
B10	0,694	0,921	0,737	0,649	degr.
C1	0,674	0,922	0,768	0,676	OCF
C3	0,675	0,920	0,767	0,675	OCF
C4	0,516	0,921	0,768	0,675	OCF
C5	0,707	0,920	0,767	0,675	degr.
C6	0,794	0,919	0,766	0,674	degr.
C7	0,611	0,922	0,769	0,676	OCF
C8	0,573	0,921	0,767	0,675	OCF
C9	0,790	0,921	0,767	0,675	degr.
C10	0,605	0,921	0,768	0,676	OCF
D2	0,682	0,922	0,768	0,676	degr.
D3	0,724	0,922	0,768	0,676	degr.
D4	0,900	0,922	0,769	0,676	degr.
D7	0,800	0,922	0,768	0,676	degr.
D8	0,656	0,922	0,768	0,676	OCF
D9	0,824	0,921	0,768	0,676	degr.
E3	0,770	0,923	0,738	0,650	degr.
E4	0,747	0,922	0,768	0,676	degr.
E6	0,764	0,921	0,737	0,649	degr.
E7	0,674	0,922	0,738	0,649	degr.
E8	0,916	0,922	0,738	0,649	degr.
E9	0,900	0,923	0,738	0,650	degr.
E10	0,951	0,922	0,738	0,649	degr.

(a). normal condition
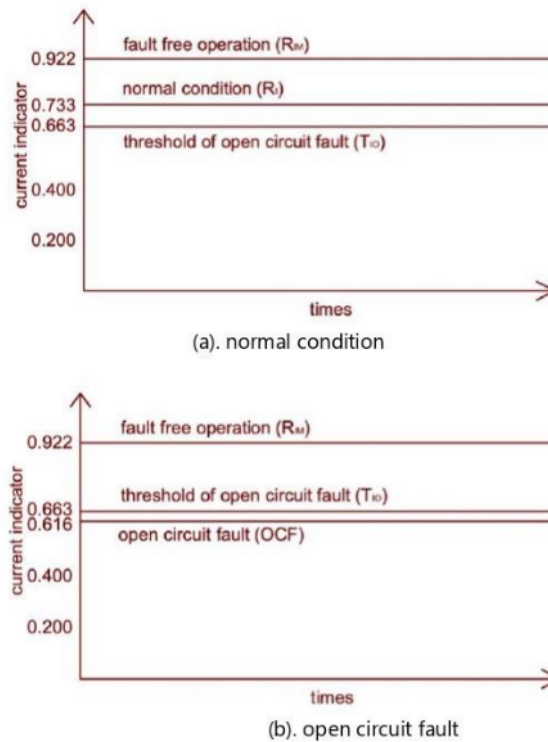
(b). open circuit fault

Fig 7. The current indicators, threshold open circuit fault (T_{IO}), normal condition (R_I) and fault free operation (RI_M) in normal condition (a), the current indicators, open circuit fault (OCF), threshold open circuit fault (T_{IO}), and fault free operation (R_{IM}) in open circuit fault (b).

Table 3 shows the data from measurements, calculations, and observations in detecting open circuit fault PV arrays. Degradation (deg.) are conditions where the real-time value of the current indicator (RI) (during operation) is greater than the open circuit fault threshold (TIO) but lower than the current indicator in fault free operation (RIM). The open circuit threshold value is 0.663, and the average current indicator (normal condition) is 0.733 above the open circuit threshold value. At the same time, the current indicator value in the fault-free operation is 0.922, the highest than the other, as shown in **Fig 7**(a).

Open current fault (OCF) are conditions where the real-time value of the current indicator (RI)(during operation) is lower than the open circuit fault threshold (TIO). The average current indicator (RI) in a fault condition is 0.616, lower than the open circuit threshold (0.663). At the same time, the current indicator in the fault-free operation is 0.922, as shown in **Fig 7**(b).

4.3 Short Circuit Fault Observation and Detection

Observation and detection of short circuit faults, from all the data that has been collected then, calculations are carried out using the equation (1), (4), (5), (8), (12), (13), (14) so that the results are as shown in Table 4. The results were obtained from 39unit boxes combiner, and it was detected that a short circuit fault (SCF) occurred in 14 combiner box units, namely the combiner boxes A2, A6, A7, B9, B10, C6, C8, C9, D2, D7, D9, E4, E6, E9. In this case, the analysis results show that the value of the voltage measurement indicator is smaller than the short circuit fault threshold.

Table 4. Result of observation and detection of short circuit fault

Box. Com.	RV	RVM	RVS	TVS	Result
A1	0,754	0,824	0,778	0,685	deg.
A2	0,649	0,825	0,779	0,685	SCF
A3	0,711	0,824	0,778	0,685	deg.
A4	0,692	0,824	0,778	0,685	deg.
A6	0,362	0,823	0,778	0,684	SCF
A7	0,634	0,823	0,778	0,684	SCF
A8	0,722	0,823	0,778	0,684	deg.
A9	0,718	0,824	0,778	0,685	deg.
A10	0,756	0,823	0,778	0,684	deg.
B1	0,726	0,824	0,778	0,685	deg.
B2	0,733	0,824	0,778	0,685	deg.
B3	0,754	0,824	0,778	0,685	deg.
B4	0,734	0,823	0,777	0,684	deg.
B5	0,702	0,824	0,778	0,685	deg.
B6	0,707	0,823	0,778	0,684	deg.
B9	0,372	0,824	0,778	0,685	SCF
B10	0,623	0,824	0,779	0,685	SCF
C1	0,694	0,824	0,778	0,685	deg.
C3	0,702	0,825	0,779	0,685	deg.
C4	0,734	0,824	0,778	0,685	deg.
C5	0,724	0,824	0,778	0,685	deg.
C6	0,429	0,824	0,779	0,685	SCF
C7	0,717	0,823	0,777	0,684	deg.
C8	0,666	0,825	0,779	0,686	SCF
C9	0,623	0,824	0,779	0,685	SCF
C10	0,714	0,824	0,778	0,685	deg.
D2	0,625	0,823	0,778	0,684	SCF
D3	0,777	0,824	0,778	0,684	deg.
D4	0,733	0,823	0,777	0,684	deg.
D7	0,627	0,824	0,778	0,684	SCF
D8	0,714	0,824	0,778	0,685	deg.
D9	0,610	0,824	0,778	0,685	SCF
E3	0,713	0,824	0,778	0,684	deg.
E4	0,606	0,824	0,778	0,685	SCF
E6	0,597	0,824	0,778	0,685	SCF
E7	0,770	0,823	0,778	0,684	deg.
E8	0,722	0,824	0,778	0,684	deg.
E9	0,577	0,824	0,778	0,684	SCF
E10	0,767	0,824	0,778	0,684	deg.

Table 4 shows the data from measurements, calculations, and observations in detecting short circuit fault PV arrays. Degradation (deg.) are conditions where the real-time of the voltage indicator (during operation) (RV) is greater than the short circuit fault threshold (TVS) but lower than the voltage indicator in fault free operation (RVM). The short circuit threshold (TVS) is 0.685, and the average voltage indicator (RV) is 0.733 above the short circuit threshold (TVS). At the same time, the voltage indicator in the fault-free operation (RVM) is 0.824, the highest than the other, as shown in **Fig 8**(a).

(a). normal condition.
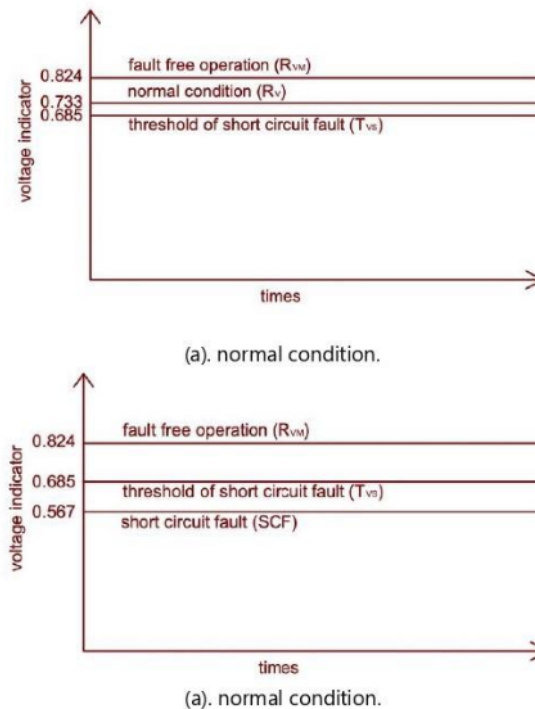
(a). normal condition.

Fig 9. The voltage indicators, threshold short circuit fault (T_{VS}), measurement (R_V), and fault free operation (R_{VM}), in normal condition (a), the voltage indicators, short circuit fault (SCF), threshold short circuit fault (T_{VS}), and fault free operation (R_{VM}) in short circuit fault (b).

Short circuit fault (S.C.F) are conditions where the voltage indicator (during operation) is lower than the short circuit fault threshold. The average voltage indicator in a fault condition is 0.584 lower than the short circuit threshold (0.700). At the same time, the voltage indicator in the fault-free operation is 0.823, as shown in **Fig 8(b).**

4.4 Degradation
The Bangli PV Power plant has been operating for nine years since 2013. The 200Wp PV module installed in Bangli has 1% degradation per year, so the degradation of the Bangli PV system after nine years of operation is 9%, or the maximum energy generation is 91%. According to the measurements and calculation results, when compared to energy generation in fault-free operation conditions, the degradation factor of Bangli PV has reduced the energy generation capacity to 86%.

5. Conclusion
Bangli PV system found short circuit and open circuit disturbances. Ten combiner box units experience open circuit problems and 14 combiner boxes that experience short circuit problems, and there is a combiner box with both problems. The effect of degradation is not considered a disturbance; degradation is a natural factor experienced by all PV modules. Meanwhile, the determination of the disturbance threshold value is the key to the accuracy of the fault determination using the current and voltage observation method.

The contribution of this study is to determine the threshold value in detecting faults using the current and voltage observation method. Previously, it was determined that fault detection allowed offset coefficient = 2% (Silvestre et al., 2014). Degradation is an essential factor that needs to be considered in determining the disturbance threshold. The degradation factor ranges between 0.5% - 1% per year. With a working life of 9 years, the PV factor of the Bangli system is set at 8%. Based on this set fault threshold, the detection of open circuit faults and open circuit faults that occur in the Bangli PV system can be determined.
Some of the limitations of this study are that data collection is carried out using measuring instruments manually and in a relatively short period. Manual data retrieval and the precision of measuring instruments that are not optimal significantly affect the results' accuracy of detection.

As a suggestion for future research, some improvements that can be made are, first, in data collection, current and voltage data should be taken directly from the output of the inverter. As for radiation data, it is better to use a pyranometer to obtain continuous and complete data. Second, in terms of research methods, it is possible to use a combination of two methods: the current and voltage observation method and the power loss analysis method. Besides that, the most urgent thing is determining the offset factor as a correction to the threshold value in determining the fault.

Conflicts of Interest: The authors declare no conflict of interest
ORCID iD: https://orcid.org/000-0002-3609-3945
Publisher's Note: All claims expressed in this article are solely those of the authors and do not necessarily represent those of their affiliated organizations or those of the publisher, the editors, and the reviewers.

References

[1]   Chen, L., Li, S., & Wang, X. (2018). Quickest Fault Detection in Photovoltaic Systems. *IEEE Transactions on Smart Grid*, *9*(3). https://doi.org/10.1109/TSG.2016.2601082

[2]   Chen, L., & Wang, X. (2018). Adaptive fault localization in photovoltaic systems. *IEEE Transactions on Smart Grid*, *9*(6). https://doi.org/10.1109/TSG.2017.2722821

[3]   Fazai, R., Abodayeh, K., Mansouri, M., Trabelsi, M., Nounou, H., Nounou, M., & Georghiou, G. E. (2019). Machine learning-based statistical testing hypothesis for fault detection in photovoltaic systems. *Solar Energy*, *190*. https://doi.org/10.1016/j.solener.2019.08.032

[4]   Firth, S. K., Lomas, K. J., & Rees, S. J. (2010). A simple model of PV system performance and its use in fault detection. *Solar Energy*, *84*(4). https://doi.org/10.1016/j.solener.2009.08.004

[5]   Harrou, F., Taghezouit, B., & Sun, Y. (2019). Robust and flexible strategy for fault detection in grid-connected photovoltaic systems. *Energy Conversion and Management*, *180*. https://doi.org/10.1016/j.enconman.2018.11.022

[6]   Jordan, D. C., & Kurtz, S. R. (2013). Photovoltaic degradation rates - An Analytical Review. In *Progress in Photovoltaics: Research and Applications* (Vol. 21, Issue 1). https://doi.org/10.1002/pip.1182

[7]   Jordan, Dirk C., Kurtz, S. R., VanSant, K., & Newmiller, J. (2016). Compendium of photovoltaic degradation rates. *Progress in Photovoltaics: Research and Applications*, *24*(7). https://doi.org/10.1002/pip.2744

[8]   Kumar, B. P., Ilango, G. S., Reddy, M. J. B., & Chilakapati, N. (2018). Online fault detection and diagnosis in photovoltaic systems using wavelet packets. *IEEE Journal of Photovoltaics*, *8*(1). https://doi.org/10.1109/JPHOTOV.2017.2770159

[9]   Lillo-Bravo, I., González-Martínez, P., Larrañeta, M., & Guasumba-Codena, J. (2018). Impact of energy losses due to failures on photovoltaic plant energy balance. *Energies*, *11*(2). https://doi.org/10.3390/en11020363

[10] Sangwongwanich, A., Yang, Y., Sera, D., & Blaabjerg, F. (2018). Lifetime Evaluation of Grid-Connected PV Inverters Considering Panel Degradation Rates and Installation Sites. *IEEE Transactions on Power Electronics*, *33*(2). https://doi.org/10.1109/TPEL.2017.2678169

[11] Silvestre, S., Silva, M. A. Da, Chouder, A., Guasch, D., & Karatepe, E. (2014). New procedure for fault detection in grid connected PV systems based on the evaluation of current and voltage indicators. *Energy Conversion and Management*, *86*. https://doi.org/10.1016/j.enconman.2014.05.008

[12] Yahyaoui, I., & Segatto, M. E. V. (2017). A practical technique for on-line monitoring of a photovoltaic plant connected to a single-phase grid. *Energy Conversion and Management*, *132*. https://doi.org/10.1016/j.enconman.2016.11.031

[13] Yi, Z., & Etemadi, A. H. (2017). Line-to-line fault detection for photovoltaic arrays based on multi-resolution signal decomposition and two-stage support vector machine. *IEEE Transactions on Industrial Electronics*, *64*(11). https://doi.org/10.1109/TIE.2017.2703681

Similarity Check-Short and Open Circuit Fault Detection in On Grid Photovoltaic Systems

Similarity Check-Short and Open Circuit Fault Detection in On Grid Photovoltaic Systems